PERGAMON

International Journal of Solids and Structures 38 (2001) 7643–7658

INTERNATIONAL JOURNAL OF SOLIDS and STRUCTURES

www.elsevier.com/locate/ijsolstr

On a plane crack in piezoelectric solids

X.-L. Xu, R.K.N.D. Rajapakse *

Department of Civil and Geological Engineering, University of Manitoba Winnipeg, Canada R3T 5V6

Received 1 December 1999

Abstract

A new analytical solution for a piezoelectric plane with an elliptical void is derived by removing the commonly held assumptions that the void boundary is impermeable and a void axis is perpendicular to the poling direction. The approach of Lekhnitskii's complex potential functions is used in the derivation. Applicability of the common practice of reducing a void solution to a crack solution is examined. It is shown that a recently reported solution for exact electric boundary conditions is actually the well known solution for a permeable crack. A unified formulation for plane cracks containing air or vacuum is then developed to account for different electric boundary conditions. Crack closure is taken into consideration in the analysis. The influence of electric boundary conditions and crack orientation on fracture parameters is discussed.

Keywords: Anisotropy; Cracks; Electric field; Fracture mechanics; Piezoelectric; Stress concentration

1. Introduction

Park et al. (1998) observed that service performance of piezoceramics is degenerated by void-like defects. The study of defects (voids, cracks, etc.) in piezoelectrics is therefore necessary to understand the failure mechanisms of such materials. By assuming an electrically impermeable boundary, Sosa (1991) examined stress concentration around an elliptical hole. Sosa and Khutoryansky (1996) revisited an identical problem by removing the assumption of an impermeable boundary. An elliptic axis was taken to be perpendicular to the poling direction in above studies. Xu and Rajapakse (1999) presented an analytical solution for an arbitrarily oriented elliptical void by assuming an electrically impermeable boundary.

A number of researchers examined crack problems in plane piezoelectrics (e.g. Parton, 1976; Suo et al., 1992). However, there are conflicting views on some key issues. For example, different electric boundary conditions have been proposed for cracks containing air or vacuum. Polovinkina and Ulitko (1978) and Mikhailov and Parton (1990) used a permeable crack model, which assumes the continuity of electric potential and the normal component of electrical displacement across the crack faces. Suo et al. (1992)

* Corresponding author. Address: Department of Mechanical Engineering, University of British Columbia, Vancouver, Canada V6T 1Z4. Tel.: +1-604-822-0497; fax: +1-604-822-0944.

E-mail address: rajapakse@mech.ubc.ca (R.K.N.D. Rajapakse).

0020-7683/01/$ - see front matter
PII: S0020-7683(01)00029-4

argued that this condition is not realistic, as there is an electric potential drop across the crack. Deeg (1980) proposed an impermeable crack model, i.e., the vanishing of normal electric displacement on the crack faces. Pak (1990) provided arguments for the validity of Deeg's model. Dunn (1994), Zhang and Tong (1996) and Zhang et al. (1998) examined the crack face boundary conditions by studying an elliptical void. By taking the limits of a void, Zhang and Tong (1996) and Zhang et al. (1998) discussed the effects of crack geometry and permittivity. They found that different limits of governing variables result in different crack face conditions. Hao and Shen (1994) proposed a new electric boundary condition by considering the electric permeability of air or vacuum in a crack.

Pak (1992) showed that an electric field generally impedes crack growth based on the criterion of total energy release rate. Employing the criterion of strain energy release rate, Park and Sun (1995a,b) reported that a positive electric field reduces the fracture load, and a negative one increases it. Kumar and Singh (1996), by using the criterion of maximum hoop stress, reported that cracks propagate less under a positive electric field and more under a negative field. Contradictory experimental findings about the effect of an applied electric field are reported in literature (Singh and Wang, 1995; Park and Sun, 1995a).

Coordinated experimental studies are needed to understand the real electric boundary condition on crack faces and to clarify the role of an applied electric field. Past theoretical studies exclusively assumed that a crack is perpendicular/parallel to the poling direction or has impermeable crack faces. In addition, limited knowledge exists on the dependence of fracture parameters on crack orientation and electric boundary conditions. The present study is also motivated by a recent study (Gao and Fan, 1999) where it is claimed that the solution for a plane crack under exact electric boundary conditions is given, and the need to closely examine the electric boundary conditions proposed by Hao and Shen (1994).

A new analytical solution for a piezoelectric plane containing an arbitrarily oriented and permeable elliptical void is first established to obtain a unified formulation for crack problems under different electric boundary conditions. Applicability of common practice of reducing void solutions to crack solutions is discussed. An alternative approach is utilized to develop a formulation which accounts for an arbitrary crack orientation and different boundary conditions. Numerical results are presented to show the influence of different electric boundary conditions and crack orientations on fracture parameters such as field intensity factors, energy release rates and crack tip hoop stress. It is shown that the solution of Gao and Fan (1999) is actually the previously known solution for a permeable crack, and the solution of Hao and Shen (1994) reduces to the solution of an impermeable or a permeable crack under practical situations.

2. Arbitrarily oriented elliptical void

Consider an infinite piezoelectric plane polarized in the z'-direction and containing an elliptical void as shown in Fig. 1. The orientation of the void (z-axis of xz system) with respect to the poling direction is arbitrary and denoted by angle β. The homogeneous domain inside the void may be vacuum or air. The void is free of electric charges, and no free charges exist on the piezoelectric–void interface.

Assuming plane stress or plane strain conditions, the constitutive equations in the xz system can be expressed as,

$$\begin{Bmatrix} \epsilon_{xx} \\ \epsilon_{zz} \\ 2\epsilon_{xz} \end{Bmatrix} = \begin{pmatrix} a_{11} & a_{12} & a_{13} \\ a_{12} & a_{22} & a_{23} \\ a_{13} & a_{23} & a_{33} \end{pmatrix} \begin{Bmatrix} \sigma_{xx} \\ \sigma_{zz} \\ \sigma_{xz} \end{Bmatrix} + \begin{pmatrix} b_{11} & b_{21} \\ b_{12} & b_{22} \\ b_{13} & b_{23} \end{pmatrix} \begin{Bmatrix} D_x \\ D_z \end{Bmatrix}$$
$$\begin{Bmatrix} E_x \\ E_z \end{Bmatrix} = -\begin{pmatrix} b_{11} & b_{12} & b_{13} \\ b_{21} & b_{22} & b_{23} \end{pmatrix} \begin{Bmatrix} \sigma_{xx} \\ \sigma_{zz} \\ \sigma_{xz} \end{Bmatrix} + \begin{pmatrix} d_{11} & d_{12} \\ d_{12} & d_{22} \end{pmatrix} \begin{Bmatrix} D_x \\ D_z \end{Bmatrix} \tag{1}$$

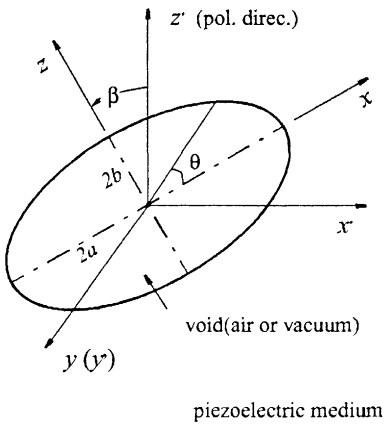

Fig. 1. An arbitrarily oriented elliptical void.

where ϵ_{ij}, σ_{ij}, D_i and E_i $(i,j=x,z)$ denote the strain tensor, stress tensor, electric displacement in the i-direction and electric field in the i-direction, respectively. Coefficients a_{ij}, b_{ij} and d_{ij} are two-dimensional elastic, piezoelectric and dielectric constants, respectively (Xu and Rajapakse, 1999). These coefficients are different for plane stress and plane strain cases, and are functions of material constants in Eq. (A.1) and void orientation angle β. The material properties of piezoceramics PZT-4 and PZT-5H are given in Appendix A.

The general solutions for plane piezoelectrics can be expressed as,

$$\begin{aligned}
\{u_x,u_z,\phi\}^{\mathrm{T}} &= 2\,\mathrm{Re}\sum_{n=1}^{3}\{p_n,q_n,s_n\}^{\mathrm{T}}\varphi_n(z_n)\\
\{\sigma_{xx},\sigma_{zz},\sigma_{xz}\}^{\mathrm{T}} &= 2\,\mathrm{Re}\sum_{n=1}^{3}\{\mu_n^2,1,-\mu_n\}^{\mathrm{T}}\varphi_n'(z_n)\\
\{D_x,D_z\}^{\mathrm{T}} &= 2\,\mathrm{Re}\sum_{n=1}^{3}\{\delta_n\mu_n,-\delta_n\}^{\mathrm{T}}\varphi_n'(z_n)\\
\{E_x,E_z\}^{\mathrm{T}} &= -2\,\mathrm{Re}\sum_{n=1}^{3}\{s_n,t_n\}^{\mathrm{T}}\varphi_n'(z_n)
\end{aligned} \tag{2}$$

where u_x, u_z and ϕ denote displacements in the x-, z-directions and electric potential, respectively; a superscript T denotes transpose of a vector; $z_n=x+\mu_n z$ where μ_n $(n=1,2,3)$ are the roots of Eq. (A.2); $\varphi_n(z_n)$ are complex potential functions; Re denotes the real part of a complex-valued quantity; a prime $(')$ denotes differentiation with respect to the corresponding argument; δ_n, p_n, q_n, s_n and t_n defined by Eqs. (A.3)–(A.7) are complex constants that depend on material properties and void orientation angle.

Air or vacuum inside the void is governed by Maxwell's equation, electric constitutive equations and electric field–potential relations. Let ε_{v} denote the dielectric permittivity of the medium inside the void, then,

$$D^{\mathrm{v}}_{i,i}=0; \qquad D^{\mathrm{v}}_i=\varepsilon_{\mathrm{v}}E^{\mathrm{v}}_i; \qquad E^{\mathrm{v}}_i=-\phi^{\mathrm{v}}_{,i} \tag{3}$$

where a superscript v is used to denote quantities associated with the void.

The general solutions for an dielectric medium governed by Eq. (3) can be expressed as,

$$\begin{aligned}
&\phi^{\mathrm{v}} = 2\,\mathrm{Im}[\psi(z_{\mathrm{v}})] \\
&D_x^{\mathrm{v}} = -2\varepsilon_{\mathrm{v}}\,\mathrm{Im}[\psi'(z_{\mathrm{v}})]; \qquad D_z^{\mathrm{v}} = -2\varepsilon_{\mathrm{v}}\,\mathrm{Re}[\psi'(z_{\mathrm{v}})] \\
&E_x^{\mathrm{v}} = -2\,\mathrm{Im}[\psi'(z_{\mathrm{v}})]; \qquad E_z^{\mathrm{v}} = -2\,\mathrm{Re}[\psi'(z_{\mathrm{v}})]
\end{aligned} \tag{4}$$

where $\psi(z_{\mathrm{v}})$ is a complex function with $z_{\mathrm{v}} = x + \mathrm{i}z$, Im denotes the imaginary part of a complex-valued quantity.

Assume uniform electroelastic loading $\sigma_{x'x'}^{\infty}$, $\sigma_{z'z'}^{\infty}$, $\sigma_{x'z'}^{\infty}$ and $D_{x'}^{\infty}$, $D_{z'}^{\infty}$ (or $E_{x'}^{\infty}$, $E_{z'}^{\infty}$) applied at far field (Fig. 1). Alternatively, the loading can be expressed as σ_{xx}^{∞}, σ_{zz}^{∞}, σ_{xz}^{∞} and D_x^{∞}, D_z^{∞} under the xz system. Let $\mathbf{n}$ (n_x, n_z) denote the outward unit normal of the void boundary. The following equations hold on the void boundary (i.e. piezoelectric–void interface).

$$\sigma_{xx}n_x + \sigma_{xz}n_z = 0; \qquad \sigma_{xz}n_x + \sigma_{zz}n_z = 0 \tag{5}$$

$$D_n = D_n^{\mathrm{v}}; \qquad \phi = \phi^{\mathrm{v}} \tag{6}$$

Note that the continuity of electric potential is equivalent to the continuity of tangential component of electric field.

The potential functions $\varphi_n(z_n)$ $(n = 1, 2, 3)$ in Eq. (2) and $\psi(z_{\mathrm{v}})$ in Eq. (4) are determined such that the prescribed boundary conditions are satisfied. The derivation can be carried out by following Sosa and Khutoryansky (1996) who considered the special case of $\beta = 0$.

Alternatively, Chen and Lai (1997) showed that the electroelastic field inside a plane inhomogeneity is uniform under uniform far-field loading. Let uniform electric fields and electric displacements inside a void are denoted by E_x^0, E_z^0 and D_x^0, D_z^0, respectively. Eq. (6) can be rewritten as

$$D_n = D_x^0 n_x + D_z^0 n_z; \qquad \phi = -E_x^0 x - E_z^0 z \tag{7}$$

The problem now reduces to determining the three unknown complex functions $\varphi_n(z_n)$ $(n = 1, 2, 3)$ in Eq. (2) and D_x^0, D_z^0 (or E_x^0, E_z^0). Construct φ_n in the form of

$$\varphi_n(z_n) = c_n z_n + \varphi_n^0(z_n); \quad \text{with } \varphi_n^0(z_n) = \sum_{k=0}^{\infty} \frac{a_k^{(n)}}{z_n^k} \tag{8}$$

where c_n are complex constants, and $\varphi_n^0(z_n)$ are holomorphic functions up to infinity with complex constants $a_k^{(n)}$.

Introduce the following mapping functions that map the exterior of an ellipse in the z_n plane into the exterior of a unit circle in the ξ_n plane (Lekhnitskii, 1963).

$$z_n = \frac{a - \mathrm{i}\mu_n b}{2}\,\xi_n + \frac{a + \mathrm{i}\mu_n b}{2}\,\frac{1}{\xi_n} \tag{9}$$

The functions $\varphi_n^0(z_n)$ and constants c_n, D_x^0 and D_z^0 can be obtained by applying far-field loading conditions and interface conditions given by Eqs. (5) and (7). Details of the derivation are omitted for brevity. The final results are given below.

$$\varphi_n^0(z_n) = \frac{z_n - \sqrt{z_n^2 - (a^2 + \mu_n^2 b^2)}}{a + \mathrm{i}\mu_n b}\,(\Lambda_{n1}Q_1 + \Lambda_{n2}Q_2 + \Lambda_{n3}Q_3); \quad (n = 1, 2, 3) \tag{10}$$

where

$$\begin{pmatrix} \Lambda_{11} & \Lambda_{12} & \Lambda_{13} \\ \Lambda_{21} & \Lambda_{22} & \Lambda_{23} \\ \Lambda_{31} & \Lambda_{32} & \Lambda_{33} \end{pmatrix} = \frac{1}{\Delta} \begin{pmatrix} \mu_2\delta_3 - \mu_3\delta_2 & \delta_2 - \delta_3 & \mu_3 - \mu_2 \\ \mu_3\delta_1 - \mu_1\delta_3 & \delta_3 - \delta_1 & \mu_1 - \mu_3 \\ \mu_1\delta_2 - \mu_2\delta_1 & \delta_1 - \delta_2 & \mu_2 - \mu_1 \end{pmatrix}$$

$$\Delta = \mu_1(\delta_2 - \delta_3) + \mu_2(\delta_3 - \delta_1) + \mu_3(\delta_1 - \delta_2) \tag{11}$$

$$Q_1 = -\frac{a\sigma_{zz}^{\infty}}{2} + \mathrm{i}\frac{b\sigma_{xz}^{\infty}}{2}; \qquad Q_2 = \frac{a\sigma_{xz}^{\infty}}{2} - \mathrm{i}\frac{b\sigma_{xx}^{\infty}}{2}; \qquad Q_3 = \frac{a(D_z^{\infty} - D_z^0)}{2} - \mathrm{i}\frac{b(D_x^{\infty} - D_x^0)}{2} \tag{12}$$

Electric displacements D_x^0 and D_z^0 are determined from,

$$\begin{aligned} &a\,\mathrm{Re}\{A_1\}D_z^0 + (b\,\mathrm{Im}\{A_1\} + a/\varepsilon_{\mathrm{v}})D_x^0 = 2\,\mathrm{Re}\{A_2\} + aE_x^{\infty} + a\,\mathrm{Re}\{A_1\}D_z^{\infty} + b\,\mathrm{Im}\{A_1\}D_x^{\infty} \\ &(a\,\mathrm{Im}\{A_1\} - b/\varepsilon_{\mathrm{v}})D_z^0 - b\,\mathrm{Re}\{A_1\}D_x^0 = 2\,\mathrm{Im}\{A_2\} + bE_z^{\infty} + a\,\mathrm{Im}\{A_1\}D_z^{\infty} - b\,\mathrm{Re}\{A_1\}D_x^{\infty} \end{aligned} \tag{13}$$

where

$$A_1 = -\sum_{n=1}^{3} s_n\Lambda_{n3}; \qquad A_2 = -\sum_{n=1}^{3} s_n(\Lambda_{n1}Q_1 + \Lambda_{n2}Q_2)$$

and c_n can be determined from

$$\begin{aligned} &-\sum_{n=1}^{3} a\,\mathrm{Re}\{c_n\} + \mathrm{i}b\,\mathrm{Re}\{c_n\mu_n\} = Q_1; \qquad -\sum_{n=1}^{3} a\,\mathrm{Re}\{c_n\mu_n\} + \mathrm{i}b\,\mathrm{Re}\{c_n\mu_n^2\} = Q_2 \\ &-\sum_{n=1}^{3} a\,\mathrm{Re}\{c_n\delta_n\} + \mathrm{i}b\,\mathrm{Re}\{c_n\delta_n\mu_n\} = Q_3 \end{aligned} \tag{14}$$

Note that only five independent equations exist in Eq. (14), and one of the six unknowns in c_n is set to zero without loss of generality.

Complex functions $\varphi_n(z_n)$ and $\varphi_n'(z_n)$ are now completely determined as

$$\varphi_n(z_n) = c_n z_n + (\Lambda_{n1}Q_1 + \Lambda_{n2}Q_2 + \Lambda_{n3}Q_3)\frac{z_n - \sqrt{z_n^2 - (a^2 + \mu_n^2 b^2)}}{a + \mathrm{i}\mu_n b} \tag{15}$$

$$\varphi_n'(z_n) = c_n + (\Lambda_{n1}Q_1 + \Lambda_{n2}Q_2 + \Lambda_{n3}Q_3)\frac{1}{a + \mathrm{i}\mu_n b}\left\{1 - \frac{z_n}{\sqrt{z_n^2 - (a^2 + \mu_n^2 b^2)}}\right\} \tag{16}$$

Substitution of Eqs. (15) and (16) into Eq. (2) yields the complete solution for electroelastic field. With D_x^0 and D_z^0 known, the electroelastic solution within the void is also completely known. Restrictions on the void orientation ($\beta = 0$) and the void boundary conditions (e.g. impermeable boundary) have been removed in the present derivation.

3. Crack solution and fracture parameters

It is a common practice to deduce the solution for a crack from a void solution by setting $b = 0$. Using Eqs. (12) and (15), the complex functions $\varphi_n(z_n)$ for the crack problem shown in Fig. 2 can be obtained as

$$\varphi_n(z_n) = c_n z_n - \frac{h_n}{2\sqrt{a}}\left(z_n - \sqrt{z_n^2 - a^2}\right) \tag{17}$$

where

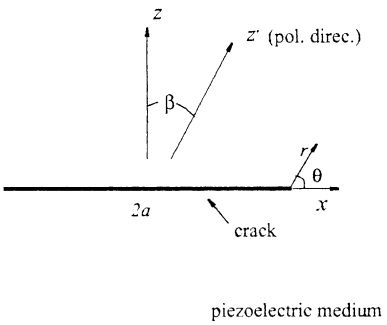

Fig. 2. An arbitrarily oriented crack.

$$h_n = \sqrt{a}\left[\Lambda_{n1}\sigma_{zz}^{\infty} - \Lambda_{n2}\sigma_{xz}^{\infty} - \Lambda_{n3}(D_z^{\infty} - D_z^0)\right]; \quad n = 1, 2, 3$$

and D_z^0 is obtained from Eq. (13) as,

$$D_z^0 = \frac{\operatorname{Im}\sum_{n=1}^{3} s_n(-\Lambda_{n1}\sigma_{zz}^{\infty} + \Lambda_{n2}\sigma_{xz}^{\infty})}{\operatorname{Im}\sum_{n=1}^{3} s_n\Lambda_{n3}} + D_z^{\infty} \tag{18}$$

Eqs. (17) and (18) based on the void solution indicate that remote electric loading has no influence on crack problems. For the special case of $\beta = 0°$, Gao and Fan (1999) made the same observation by setting $b = 0$ in their void solution. They concluded that such a solution is exact with respect to electric boundary conditions and should be used when solving fracture problems in piezoelectric materials.

The applicability of above reduction should be examined. In the case of elastic solids, such a reduction is reliable since the crack boundary conditions are consistent with the void boundary conditions (vanishing tractions). However, when dealing with piezoelectric solids such a reduction has to be carefully applied. When letting $b = 0$, the air phase physically vanishes. Consequently, the following continuities of electrical potential and normal electric displacement across the crack faces are automatically established.

$$D_z^+ = D_z^-; \qquad \phi^+ = \phi^- \tag{19}$$

where the superscripts + and − indicate the upper and lower crack surfaces, respectively.

Cracks described by Eq. (19) are referred to as permeable cracks in literature. This type of crack face electric conditions were initially proposed by Polovinkina and Ulitko (1978). In fact, Eq. (19) implies that a crack has no impact on the electric field. Therefore, in contrary to the conclusion of Gao and Fan (1999), the crack solution given by Eq. (17) is not the solution for exact electric boundary conditions. It yields the already known solution for a permeable crack as shown in the sequel.

Zhang and Tong (1996) presented an interesting discussion on reducing void solutions to crack solutions. They introduced two dimensionless parameters (functions of crack geometry and permittivity) to examine different limit solutions. It was found that permeable cracks and impermeable cracks correspond to two different limiting cases. Such a scheme, however, is not utilized here. This study aims at closely examining three existing crack models including a permeable crack, an impermeable crack and a Hao and Shen type crack.

Deeg (1980), Pak (1992) and Suo et al. (1992) assumed that crack faces are impermeable, i.e.

$$D_z^+ = D_z^- = 0 \tag{20}$$

Hao and Shen (1994) argued that neither Eq. (19) nor Eq. (20) could avoid being one-sided. By considering the electrical permeability of air or vacuum in a crack, they proposed the following electric conditions on crack faces.

$$D_z^+ = D_z^-; \qquad D_z^+(u_2^+ - u_2^-) = \varepsilon_v(\phi^- - \phi^+) \tag{21}$$

For the special case of $\varepsilon_v = 0$, i.e. a medium having zero permittivity, Eq. (21) reduces to the conditions for an impermeable crack. If potential jump $(\phi^+ - \phi^-)$ is zero, Eq. (21) reduces to the case of a permeable crack. The influence of crack face conditions expressed by Eq. (21) on fracture parameters is not clear from the analysis given by Hao and Shen (1994). Limited numerical results given by them shed little insight into the effects of Eq. (21).

A unified formulation that accounts for different electric boundary conditions (Eqs. (19)–(21)) is developed in the present study for an arbitrarily oriented crack. This new solution allows the theoretical treatment of cracks in piezoelectrics by using a single analysis. The three types of electric boundary conditions commonly assume that the normal electric displacement is continuous across the crack faces. The electric field has been shown uniform (special case of an elliptical void) under uniform loading. Therefore,

$$D_z^+ = D_z^- = D_z^0 \tag{22}$$

where D_z^0 is a constant.

Following relations can be obtained by using Eqs. (2) and (22) and vanishing tractions on crack faces.

$$2\,\mathrm{Re}\sum_{n=1}^{3}\varphi_n(x) = 0; \qquad 2\,\mathrm{Re}\sum_{n=1}^{3}\mu_n\varphi_n(x) = 0; \qquad 2\,\mathrm{Re}\sum_{n=1}^{3}\delta_n\varphi_n(x) = -D_z^0 x \tag{23}$$

where x is along the crack line $(-a \leqslant x \leqslant a)$, and the complex functions φ_n $(n = 1, 2, 3)$ are in the form of Eq. (8).

Applying the mapping of Eq. (9), $\varphi_n(z_n)$ identical to Eq. (17) are obtained. Crack tip fields can be expressed by using the polar coordinate system (r, θ) in Fig. 2 as,

$$\begin{aligned}
&\{u_x(r,\theta), u_z(r,\theta), \phi(r,\theta)\}^{\mathrm{T}} = \sqrt{2r}\,\mathrm{Re}\sum_{n=1}^{3}\{p_n, q_n, s_n\}^{\mathrm{T}} h_n\sqrt{\cos\theta + \mu_n\sin\theta}\\
&\{\sigma_{xx}(r,\theta), \sigma_{zz}(r,\theta), \sigma_{xz}(r,\theta)\}^{\mathrm{T}} = \frac{1}{\sqrt{2r}}\mathrm{Re}\sum_{n=1}^{3}\{\mu_n^2, 1, -\mu_n\}^{\mathrm{T}}\frac{h_n}{\sqrt{\cos\theta + \mu_n\sin\theta}}\\
&\{D_x(r,\theta), D_z(r,\theta)\}^{\mathrm{T}} = \frac{1}{\sqrt{2r}}\mathrm{Re}\sum_{n=1}^{3}\{\delta_n\mu_n, -\delta_n\}^{\mathrm{T}}\frac{h_n}{\sqrt{\cos\theta + \mu_n\sin\theta}}\\
&\{E_x(r,\theta), E_z(r,\theta)\}^{\mathrm{T}} = -\frac{1}{\sqrt{2r}}\mathrm{Re}\sum_{n=1}^{3}\{s_n, t_n\}^{\mathrm{T}}\frac{h_n}{\sqrt{\cos\theta + \mu_n\sin\theta}}
\end{aligned} \tag{24}$$

Eq. (24) implies that classical inverse square root type singularity exists for stresses and electric displacements irrespective of the crack orientation angle and the type of electric boundary conditions.

Crack opening displacements (COD) and the jump of electric potential along the crack line $(-a \leqslant x \leqslant a)$ can be obtained as,

$$\begin{aligned}
u_x^+ - u_x^- &= -2\sqrt{a^2 - x^2}\ \mathrm{Im}\sum_{n=1}^{3} p_n\left[\Lambda_{n1}\sigma_{zz}^{\infty} - \Lambda_{n2}\sigma_{xz}^{\infty} - \Lambda_{n3}(D_z^{\infty} - D_z^0)\right]\\
u_z^+ - u_z^- &= -2\sqrt{a^2 - x^2}\ \mathrm{Im}\sum_{n=1}^{3} q_n\left[\Lambda_{n1}\sigma_{zz}^{\infty} - \Lambda_{n2}\sigma_{xz}^{\infty} - \Lambda_{n3}(D_z^{\infty} - D_z^0)\right]\\
\phi^+ - \phi^- &= -2\sqrt{a^2 - x^2}\ \mathrm{Im}\sum_{n=1}^{3} s_n\left[\Lambda_{n1}\sigma_{zz}^{\infty} - \Lambda_{n2}\sigma_{xz}^{\infty} - \Lambda_{n3}(D_z^{\infty} - D_z^0)\right]
\end{aligned} \tag{25}$$

The problem now reduces to determining the constant D_z^0. An additional condition other than Eq. (22) must be considered. Apparently, this condition comes from Eqs. (19)–(21) for permeable, impermeable and the Hao and Shen type cracks, respectively.

For an impermeable crack, substituting $D_z^0 = 0$ into Eq. (24) yields the complete electroelastic fields.

For a permeable crack (Eq. (19)), D_z^0 is obtained by vanishing of the electric potential jump expressed by Eq. (25). The result is identical to D_z^0 given by Eq. (18). Therefore, the exact solution claimed by Gao and Fan (1999) is indeed the solution for a permeable crack.

For a Hao and Shen type crack, the following solution for D_z^0 can be obtained by using Eqs. (21) and (25).

$$D_z^0 = -\varepsilon_v \frac{\operatorname{Im}\sum_{n=1}^{3} s_n\left[\Lambda_{n1}\sigma_{zz}^{\infty} - \Lambda_{n2}\sigma_{xz}^{\infty} - \Lambda_{n3}(D_z^{\infty} - D_z^0)\right]}{\operatorname{Im}\sum_{n=1}^{3} q_n\left[\Lambda_{n1}\sigma_{zz}^{\infty} - \Lambda_{n2}\sigma_{xz}^{\infty} - \Lambda_{n3}(D_z^{\infty} - D_z^0)\right]} \tag{26}$$

Eqs. (18) and (26) show that, in contrast to vanishing D_z^0 for impermeable cracks, permeable and the Hao and Shen type cracks generally result in non-zero crack face electric displacements. Both far field mechanical and electric loading may contribute to D_z^0. Note Eq. (26) is a quadratic of D_z^0 (except for $\varepsilon_v = 0$), and two real or complex roots may exist. D_z^0 should be uniquely determined for a given piezoelectric material and loading. This issue was not discussed by Hao and Shen (1994).

If the remote electric loading is an electric field instead of an electric displacement, D_z^{∞} in crack solutions given by Eqs. (18), (24)–(26) is replaced by,

$$D_z^{\infty} = \frac{1}{d_{11}d_{22} - d_{12}^2}\left[d_{11}E_z^{\infty} - d_{12}E_x^{\infty} + (b_{21}d_{11} - b_{11}d_{12})\sigma_{xx}^{\infty} + (b_{22}d_{11} - b_{12}d_{12})\sigma_{zz}^{\infty} + (b_{23}d_{11} - b_{13}d_{12})\sigma_{xz}^{\infty}\right] \tag{27}$$

Eq. (27) indicates that loading σ_{xx}^{∞} and E_x^{∞} may have an effect on the crack solution.

Along the self-similar plane of a crack ($\theta = 0$),

$$\sigma_{zz}(r,0) = \frac{\sqrt{a}}{\sqrt{2r}}\sigma_{zz}^{\infty}; \qquad \sigma_{xz}(r,0) = \frac{\sqrt{a}}{\sqrt{2r}}\sigma_{xz}^{\infty}; \qquad D_z(r,0) = \frac{\sqrt{a}}{\sqrt{2r}}(D_z^{\infty} - D_z^0) \tag{28}$$

Stress intensity factors K_I, K_{II} and electric displacement intensity factor K_D can be expressed as (Suo et al., 1992),

$$K_I = \sqrt{\pi a}\sigma_{zz}^{\infty}; \qquad K_{II} = \sqrt{\pi a}\sigma_{xz}^{\infty}; \qquad K_D = \sqrt{\pi a}(D_z^{\infty} - D_z^0) \tag{29}$$

Eq. (29) shows that K_I and K_{II} are identical for the three types of electric boundary conditions, but K_D is different.

Energy release rate on the crack line ($\theta = 0$) can be obtained by using crack closure integral. For piezoelectric problems, the total energy is the sum of mechanical (strain) energy and electrical energy. Suppose a crack extends by a small amount δa, the total energy release rate can be expressed as,

$$G = \lim_{\delta a \to 0} \frac{1}{2\,\delta a}\int_0^{\delta a}\{\sigma_{iz}(x,0)u_i(\delta a - x, \pm\pi) + D_z(x,0)\phi(\delta a - x, \pm\pi)\}\,\mathrm{d}x \tag{30}$$

where $i = x$, z; $u_i(\delta a - x, \pm\pi) \equiv u_i(\delta a - x, \pi) - u_i(\delta a - x, -\pi)$ denotes displacement jump across the crack (COD); $\phi(\delta a - x, \pm\pi)$ denotes electric potential jump; the first part of the integral contributes to the mechanical energy release rate (G^M), the second part to the electric energy release rate (G^E), and the total energy release rate $G = G^M + G^E$.

In the case of far-field uniform stresses and electric displacements (σ_{xx}^{∞}, σ_{zz}^{∞}, σ_{xz}^{∞} and D_x^{∞}, D_z^{∞}),

$$G^{\mathrm{M}} = \frac{\pi a}{2}\left[-\operatorname{Im}\sum_{n=1}^{3} q_n \Lambda_{n1}(\sigma_{zz}^{\infty})^2 + \operatorname{Im}\sum_{n=1}^{3} p_n \Lambda_{n2}(\sigma_{xz}^{\infty})^2 + \operatorname{Im}\sum_{n=1}^{3}(q_n\Lambda_{n2} - p_n\Lambda_{n1})\sigma_{zz}^{\infty}\sigma_{xz}^{\infty} + \operatorname{Im}\sum_{n=1}^{3} p_n \Lambda_{n3}\sigma_{xz}^{\infty}(D_z^{\infty} - D_z^0) + \operatorname{Im}\sum_{n=1}^{3} q_n \Lambda_{n3}\sigma_{zz}^{\infty}(D_z^{\infty} - D_z^0)\right] \tag{31}$$

$$G^{\mathrm{E}} = \frac{\pi a}{2}\left[-\operatorname{Im}\sum_{n=1}^{3} s_n \Lambda_{n1}\sigma_{zz}^{\infty}(D_z^{\infty} - D_z^0) + \operatorname{Im}\sum_{n=1}^{3} s_n \Lambda_{n2}\sigma_{xz}^{\infty}(D_z^{\infty} - D_z^0) + \operatorname{Im}\sum_{n=1}^{3} s_n \Lambda_{n3}(D_z^{\infty} - D_z^0)^2\right] \tag{32}$$

Note the appearance of terms such as $\sigma_{zz}^{\infty}\sigma_{xz}^{\infty}$ and $\sigma_{xz}^{\infty}(D_z^{\infty} - D_z^0)$ in Eqs. (31) and (32) are due to the simultaneous presence of σ_{zz}^{∞}, σ_{xz}^{∞} and D_z^{∞}. If σ_{zz}^{∞} is the only non-vanishing far-field mechanic loading, Eqs. (31) and (32) give the energy release rates for Mode I crack problems.

Energy release rates are available for an impermeable crack perpendicular to the poling direction ($\beta = 0$) in PZT-4 and PZT-5H (Park and Sun, 1995a; Pak, 1992; Zhang et al., 1998). Setting $\beta = 0$ and using the material properties given in Appendix A, G^{M} and G calculated by Eqs. (31) and (32) are identical (up to the numerical accuracy) to the results reported in literature.

Hoop stress at the crack tip is another important parameter in fracture mechanics, especially for brittle solids. It can be shown that,

$$\sigma_{\theta\theta} = \frac{\sqrt{a}}{\sqrt{2r}}\operatorname{Re}\sum_{n=1}^{3}\left[\Lambda_{n1}\sigma_{zz}^{\infty} - \Lambda_{n2}\sigma_{xz}^{\infty} - \Lambda_{n3}(D_z^{\infty} - D_z^0)\right](\cos\theta + \mu_n \sin\theta)^{3/2} \tag{33}$$

4. Numerical results and discussion

Numerical results are presented to portray the effects of electric boundary conditions and crack orientation on fracture parameters such as field intensity factors, energy release rates and hoop stress. The role of an applied electric field is examined. The medium within a crack is a vacuum with $\varepsilon_{\mathrm{v}} = \varepsilon_0 = 8.85 \times 10^{-12}$ C^2/N m^2. Plane strain conditions are assumed. Two piezoceramics, namely PZT-4 and PZT-5H, are used in the numerical study.

The solution for D_z^0 (normal electric displacement on crack faces) obtained from Eq. (26) is discussed first. Eq. (26) generally has two real or complex roots for D_z^0, while only a real value is physically admissible. Numerical studies show that the discriminant of Eq. (26) are positive for all considered cases. Hence two distinct real roots exist. Let root 1 and root 2 denote the roots with positive and negative signs before the discriminant, respectively. Table 1 presents the two roots (i.e. D_z^0) for a crack perpendicular to the poling direction, under applied stress $\sigma_{zz}^{\infty} = 1.0$ MPa and different applied electric displacements ($D_z^{\infty} = 2.0 \times 10^{-4}$ C/m^2, 0 and -2.0×10^{-4} C/m^2). For PZT-4, the three cases of electric displacement loading result in identical values for root 1 and distinctly different values for root 2. It is unlikely that electric loading has no effect on the crack face electric field under the boundary condition given by Eq. (21). This suggests that root 1 may not be admissible. The results for PZT-5H is similar to those of PZT-4. Another evidence of admissibility of root 2 comes from Hill's boundary element results (Hill, 1997). Under the same conditions as in Table 1, Hill performed iterations based on Eq. (21) to compute D_z^0 for a penny shaped crack in PZT-4. The final converged values are unique and are closer to root 2 in Table 1. Table 2 presents the strain energy release rate (G^{M}) and the total energy release rate (G) for a Hao and Shen type crack in PZT-4 ($\beta = 0$)

Table 1
Normal electric displacement on crack faces based on Eq. (26) ($\beta = 0$)

Loading ($\sigma_{zz}^{\infty} = 1.0$ MPa)	PZT-4		PZT-5H	
	D_z^0 (root 1)	D_z^0 (root 2)	D_z^0 (root 1)	D_z^0 (root 2)
$D_z^{\infty} = 2.0 \times 10^{-4}$	3.598×10^{-2}	-5.173×10^{-5}	3.241×10^{-2}	-7.547×10^{-5}
$D_z^{\infty} = 0.0$	3.598×10^{-2}	-2.460×10^{-4}	3.323×10^{-2}	-2.663×10^{-4}
$D_z^{\infty} = -2.0 \times 10^{-4}$	3.598×10^{-2}	-4.403×10^{-4}	3.322×10^{-2}	-4.573×10^{-4}

Table 2
Energy release rates based on Eq. (26) for a crack in PZT-4 ($\beta = 0, E_z^{\infty} = 0$)

Loading (MPa)	G^{M} (root 1)	G^{M} (root 2)	G (root 1)	G (root 2)
$\sigma_{zz}^{\infty} = 0.0$	0.0	0.0	-1.677×10^{5}	0.0
$\sigma_{zz}^{\infty} = 0.2$	-2.431×10^{2}	1.451	-1.697×10^{5}	1.452
$\sigma_{zz}^{\infty} = 0.5$	-6.078×10^{2}	9.070	-1.728×10^{5}	9.070
$\sigma_{zz}^{\infty} = 0.8$	-9.727×10^{2}	23.217	-1.759×10^{5}	23.224
$\sigma_{zz}^{\infty} = 1.0$	-1.216×10^{3}	36.274	-1.780×10^{5}	36.287

under pure mechanical loading σ_{zz}^{∞} (MPa). It is found that far field tension (including zero) results in non-positive G^{M} and negative G corresponding to root 1. Again, this is physically unrealistic. The case of $\beta \neq 0°$ is also examined, and the behavior of roots is similar to $\beta = 0$. Therefore, it can be concluded that the admissible root of Eq. (26) is the one that has a negative sign before the discriminant.

It is important to check the condition for an open crack as past studies neglected this aspect. For an open crack, the z-component of crack opening displacements given by Eq. (25) should not be negative. Obviously, for a given far field tensile stress, permeable cracks (Eq. (19)) meet this condition regardless of the value of applied electric field. A Hao and Shen type crack is found to be open under an applied electric field or a tensile stress, irrespective of the electric field direction and crack orientation. An impermeable crack remains open under a pure positive electric field. Crack closure occurs under a pure negative electric field except when $\beta = 90°$. Under combined tension and negative electric field, a critical value of load ratio ($E_z^{\infty}/\sigma_{zz}^{\infty}$ V m/N) corresponding to crack closure exists for different crack orientations. The critical values of load ratio for PZT-4 are 0.1026, 0.1060, 0.1150 and 0.1420 for $\beta = 0°$, 30°, 45° and 60°, respectively. A crack remains open only for load ratios that are less than the critical values. The condition of an open crack is satisfied by all cases considered in the ensuing computations.

Fig. 3 shows $K_D/\sqrt{a}$ (C/m^2) under varying electric field for different electric boundary conditions and $\sigma_{zz}^{\infty} = 0.6$ MPa. Three crack orientation angles, i.e. $\beta = 0°$, 30° and 90° in PZT-4 are considered. As expected, K_D is independent of electric loading for a permeable crack. A relatively weak effect of β on K_D is observed for impermeable cracks, and K_D varies linearly with E_z^{∞}. When $\beta = 0°$ or 30°, the Hao and Shen type cracks and permeable cracks have nearly identical K_D, which are significantly different from K_D of impermeable cracks. When $\beta = 90°$, impermeable cracks and the Hao and Shen type cracks have identical K_D, whereas permeable cracks show vanishing K_D.

In the case of the Hao and Shen type cracks, K_D corresponding to $\beta = 90°$ is significantly different from that for $\beta \neq 90°$. This behavior is due to the quadratic term $\mathrm{Im}\sum_{n=1}^{3} q_n \Lambda_{n3}$ appearing in Eq. (26). For PZT-4 when $\beta = 90°$, this term is vanishingly small. For example, the values are 2.214×10^{-2}, 1.918×10^{-2}, 3.845×10^{-3}, 1.932×10^{-4}, -6.720×10^{-18} for $\beta = 0°$, 30°, 80°, 89.5° and 90° respectively. The linear term of Eq. (26) is generally negative. Since the admissible root is the one that has a negative sign before the discriminant, $D_z^0 \simeq 0$ is obtained for $\beta = 90°$. As a result, the Hao and Shen type cracks based on Eq. (21) have identical behavior as impermeable cracks. This observation is also confirmed by numerical results for energy release rates and hoop stresses given below.

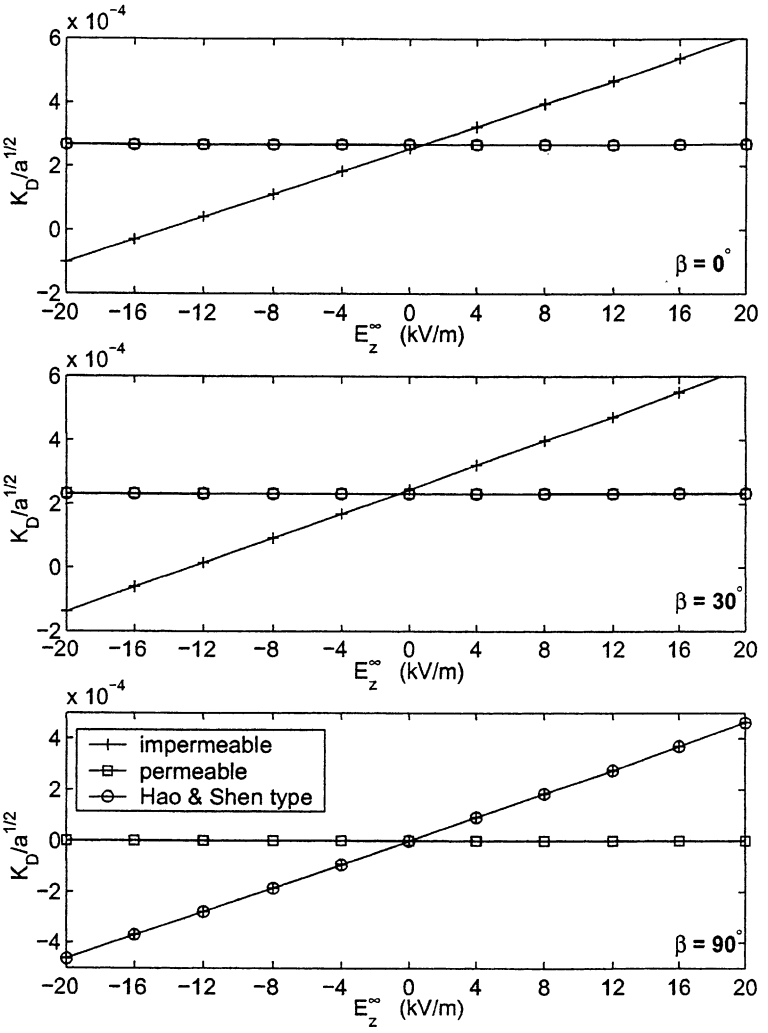

Fig. 3. Variation of electric displacement intensity factor with electric field for a crack in PZT-4 under tensile stress ($\sigma_{zz}^{\infty} = 0.6$ MPa).

Fig. 4 shows the strain energy release rate G^{M}/a (N/m^2) for PZT-4 under varying electric field and $\sigma_{zz}^{\infty} = 0.6$ MPa. Five values of crack orientation angle, i.e. $\beta = 0°$, 30°, 45°, 60° and 90°, are considered. A strong influence of crack orientation on G^{M} is observed. For all three types of electric boundary conditions, G^{M} decreases as β becomes larger except for an impermeable crack and $E_z^{\infty} \leqslant -10$ kV/m. When applied loading is pure mechanical ($E_z^{\infty} = 0$), G^{M} is independent of electric boundary conditions for any β. As expected, the applied electric field has no effect on G^{M} for a permeable crack. For an impermeable crack, G^{M} increases with E_z^{∞} when $\beta \neq 90°$ and has no effect on G^{M} when $\beta = 90°$. The dependence of G^{M} on E_z^{∞} decreases as β increases. Both permeable cracks and the Hao and Shen type cracks have nearly identical G^{M} values that are practically independent of E_z^{∞}. Strain energy release rate of a crack parallel to polarization is independent of E_z^{∞} and electric boundary conditions.

Total energy release rate G for a permeable crack is identical to G^{M} shown in Fig. 4. G/a for impermeable cracks and the Hao and Shen type cracks based on Eq. (21) are presented in Fig. 5. For

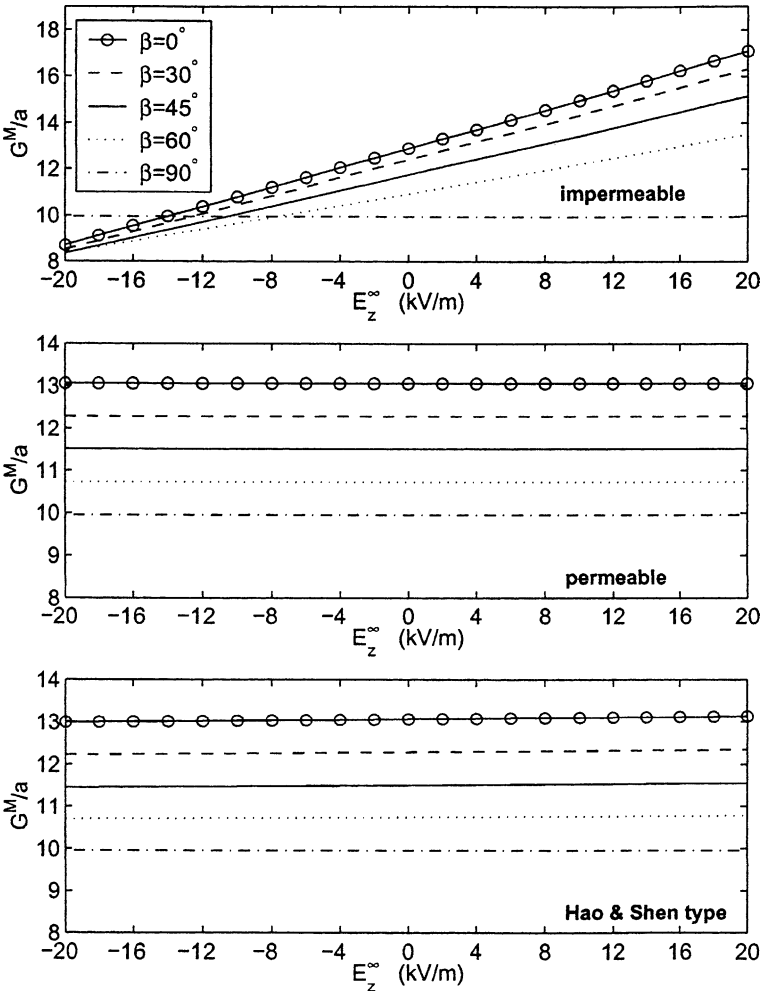

Fig. 4. Variation of strain energy release rate with electric field for a crack in PZT-4 under tensile stress ($\sigma_{zz}^{\infty} = 0.6$ MPa).

impermeable cracks, an applied electric field tends to decrease G with increasing β. For the Hao and Shen type cracks, an electric field has no effect on G when $\beta \neq 90°$. Again, the Hao and Shen type cracks and impermeable cracks show virtually identical G values when $\beta = 90°$. Total energy release rate is not symmetric with respect to E_z^{∞} for impermeable cracks when remote tension is non-zero.

Based on the criterion of strain energy release rate, an increasing β generally increases the fracture load for all three types of electric boundary conditions. An applied electric field has no effect on fracture of impermeable cracks parallel to the poling direction ($\beta = 90°$), and permeable and the Hao and Shen type cracks of arbitrary orientations. When $\beta \neq 90°$, a positive electric field tends to enhance extension of an impermeable crack and a negative one tends to retard it. Applying the criterion of total energy release rate, the fracture load increases with increasing β regardless of electric boundary conditions, which is similar to the behaviour of G^{M}. For arbitrarily oriented impermeable cracks and the Hao and Shen type cracks perpendicular to the poling direction, both positive and negative electric fields tend to impede crack growth. For the Hao and Shen type cracks not perpendicular to the poling direction, an applied electric field has no influence on their fracture behavior.

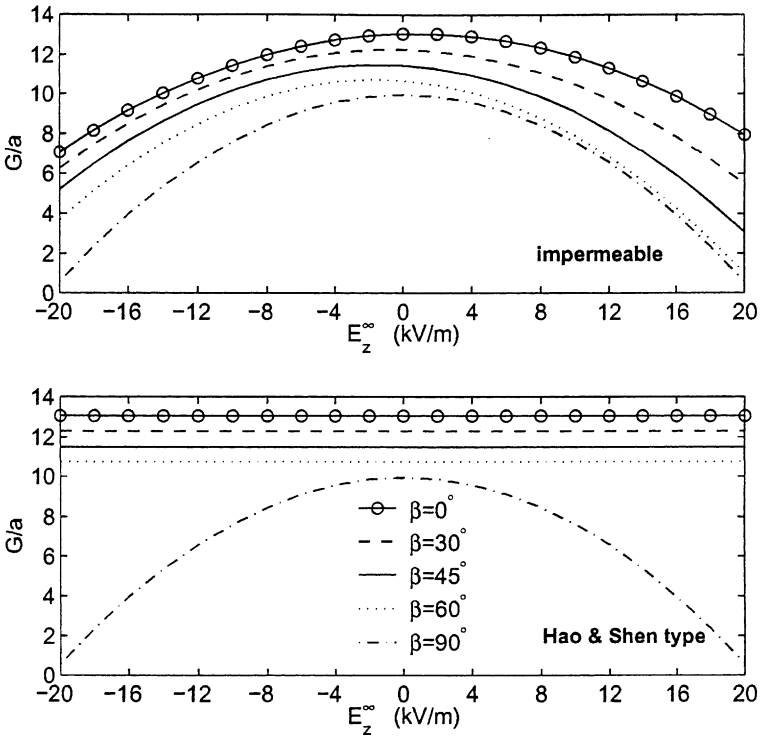

Fig. 5. Variation of total energy release rate with electric field for a crack in PZT-4 under tensile stress ($\sigma_{zz}^\infty = 0.6$ MPa).

Hoop stress distribution at a crack tip is now considered. Under pure tensile loading σ_{zz}^∞, hoop stress profiles are found to be virtually independent of electric boundary conditions and crack orientation angle β. Numerical results are not shown for brevity. Fig. 6 shows the variation of normalized hoop stress $\sqrt{2r/a}\sigma_{\theta\theta}/E_z^\infty$ (N/V m) under a pure positive electric field E_z^∞ in PZT-4. For a permeable crack, a pure electric field has no contribution to hoop stress, which is obvious from Eqs. (17) and (18). For an impermeable crack, hoop stress distribution depends significantly on β. Compressive hoop stresses are observed at the entire crack tip when $\beta = 0°$, while tensile stresses are observed when $\beta = 60°$. Both compressive and tensile stresses exist for $\beta = 30°$, 45° and 90°. Again, a Hao and Shen type crack has practically same $\sigma_{\theta\theta}$ as a permeable crack for $\beta \neq 90°$, and identical $\sigma_{\theta\theta}$ as an impermeable crack when $\beta = 90°$.

Following the criterion of maximum hoop stress, fracture initiation and crack branching are generally expected for an impermeable crack, with the exception of the case $\beta = 0°$. For a Hao and Shen type crack, crack extension and branching are expected only when the crack is perpendicular to the poling direction. The observation that impermeable cracks and the Hao and Shen type cracks may deviate from a straight line for certain crack orientations is consistent with the experimental phenomenon of crack skewing (McHenry and Koepke, 1983).

5. Conclusions

Removing the assumption of an impermeable void boundary and the restriction on void orientation, a new analytical solution is obtained for a piezoelectric plane with an elliptical void. It is shown that the exact

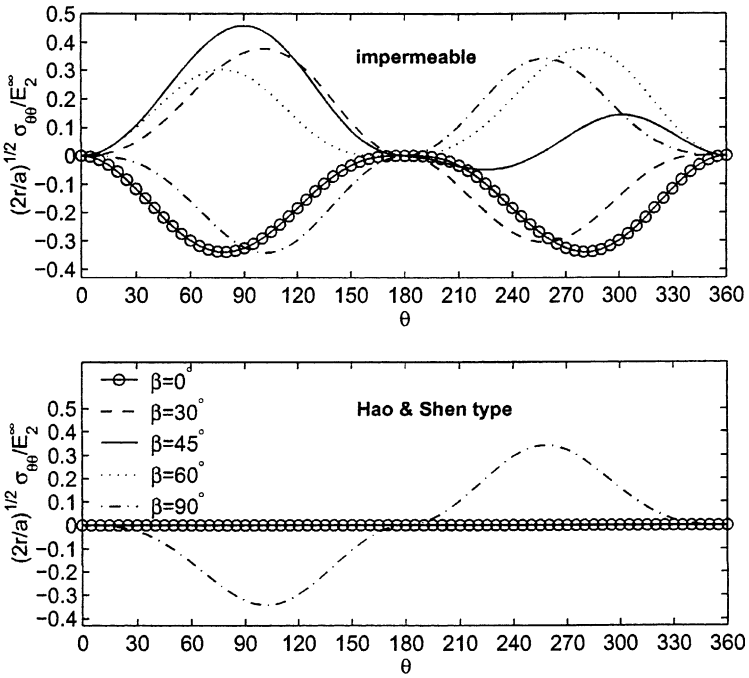

Fig. 6. Variation of crack tip hoop stresses in PZT-4 under applied positive electric field.

crack boundary condition solution reported previously by others is actually the solution for a permeable crack. A unified formulation accounting for three existing types of electric boundary conditions is developed for arbitrarily oriented cracks. It is found that electric boundary conditions practically have no effect on fracture parameters under pure mechanical loading. The Hao and Shen type cracks and permeable cracks with $\beta \neq 90°$ have virtually identical fracture behavior that is practically independent of applied electric loading. However, for cracks parallel to the poling direction, the Hao and Shen type cracks behave as impermeable cracks. A substantial dependence of the crack tip hoop stress on crack orientations is noted for impermeable cracks. Tensile hoop stresses are observed for $\beta \neq 0°$. The criterion of maximum hoop stress can explain experimentally observed crack skewing. Energy release rates generally decrease with increasing β. Energy release rates along the self-similar line, being not able to account for crack deviation, may not qualify as potential fracture criteria. A study of energy release rates for arbitrary crack extension directions would be useful.

Acknowledgements

The work presented in this paper was supported by the Natural Sciences and Engineering Research Council of Canada grant A-6507.

Appendix A

The constitutive equations for z'-polarized ceramics in the $x'y'z'$ system can be expressed as (Parton and Kudryavtsev, 1988)

$$[\sigma'] = [c][\epsilon'] - [e]^{\mathrm{T}}[E']; \qquad [D'] = [e][\epsilon'] + [\varepsilon][E'] \tag{A.1}$$

where a prime denotes variables with respect to the $x'y'z'$ system; c_{ij}, e_{ij} and ε_{ij} denote elastic constants, piezoelectric constants and dielectric constants, respectively.

μ_n are the roots of the characteristic equation,

$$P(\mu) = l_1(\mu)l_3(\mu) + l_2^2(\mu) = 0 \tag{A.2}$$

with

$$l_1(\mu) = d_{11}\mu^2 - 2d_{12}\mu + d_{22}; \qquad l_2(\mu) = b_{11}\mu^3 - (b_{21} + b_{13})\mu^2 + (b_{12} + b_{23})\mu - b_{22}$$
$$l_3(\mu) = a_{11}\mu^4 - 2a_{13}\mu^3 + (2a_{12} + a_{33})\mu^2 - 2a_{23}\mu + a_{22}$$

The roots (μ) of Eq. (A.2) are complex with three pair wise conjugates, and they are generally distinct. Note μ_n ($n = 1, 2, 3$) in Eq. (2) are chosen such that their imaginary parts are positive.

The constants δ_n, p_n, q_n, s_n and t_n in Eq. (2) are

$$\delta_n = l_2(\mu_n)/l_1(\mu_n) \tag{A.3}$$

$$p_n = a_{11}\mu_n^2 + a_{12} - a_{13}\mu_n + \delta_n(b_{11}\mu_n - b_{21}) \tag{A.4}$$

$$q_n = (a_{12}\mu_n^2 + a_{22} - a_{23}\mu_n + \delta_n b_{12}\mu_n - \delta_n b_{22})/\mu_n \tag{A.5}$$

$$s_n = b_{11}\mu_n^2 + b_{12} - b_{13}\mu_n - \delta_n(d_{11}\mu_n - d_{12}) \tag{A.6}$$

$$t_n = b_{21}\mu_n^2 + b_{22} - b_{23}\mu_n - \delta_n(d_{12}\mu_n - d_{22}) \tag{A.7}$$

The material properties of PZT-4 and PZT-5H based on Eq. (A.1) are given below. PZT-4 (Park and Sun, 1995b):

$$c_{11} = 13.9 \times 10^{10}\ \mathrm{N/m^2}, \quad c_{12} = 7.78 \times 10^{10}\ \mathrm{N/m^2}, \quad c_{13} = 7.43 \times 10^{10}\ \mathrm{N/m^2}$$
$$c_{33} = 11.3 \times 10^{10}\ \mathrm{N/m^2}, \qquad c_{44} = 2.56 \times 10^{10}\ \mathrm{N/m^2}$$
$$e_{31} = -6.98\ \mathrm{C/m^2}, \quad e_{33} = 13.84\ \mathrm{C/m^2}, \quad e_{15} = 13.44\ \mathrm{C/m^2}$$
$$\varepsilon_{11} = 6.00 \times 10^{-9}\ \mathrm{CV/m}, \qquad \varepsilon_{33} = 5.47 \times 10^{-9}\ \mathrm{CV/m}$$

PZT-5H (Pak, 1992):

$$c_{11} = 12.6 \times 10^{10}\ \mathrm{N/m^2}, \quad c_{12} = 5.5 \times 10^{10}\ \mathrm{N/m^2}, \quad c_{13} = 5.3 \times 10^{10}\ \mathrm{N/m^2}$$
$$c_{33} = 11.7 \times 10^{10}\ \mathrm{N/m^2}, \qquad c_{44} = 3.53 \times 10^{10}\ \mathrm{N/m^2}$$
$$e_{31} = -6.5\ \mathrm{C/m^2}, \quad e_{33} = 23.3\ \mathrm{C/m^2}, \quad e_{15} = 17.0\ \mathrm{C/m^2}$$
$$\varepsilon_{11} = 151 \times 10^{-10}\ \mathrm{CV/m}, \qquad \varepsilon_{33} = 130 \times 10^{-10}\ \mathrm{CV/m}$$

References

Chen, T., Lai, D., 1997. An exact correspondence between plane piezoelectricity and generalized plane strain in elasticity. Proceeding of the Royal Society, London Series A, vol. 453, pp. 2689–2713.

Deeg, W.F., 1980. The analysis of dislocation, crack and inclusion problems in piezoelectric solids. Ph.D. Thesis, Standford University, USA.

Dunn, M.L., 1994. The effects of crack face boundary conditions on the fracture mechanics of piezoelectric solids. Engineering Fracture Mechanics 48, 25–39.

Gao, C.-F., Fan, W.-X., 1999. Exact solutions for the plane problem in piezoelectric materials with an elliptic or a crack. International Journal of Solids and Structures 36, 2527–2540.

Hao, T.-H., Shen, Z.-Y., 1994. A new electric boundary condition of electric fracture mechanics and its applications. Engineering Fracture Mechanics 47, 793–802.

Hill, L.S., 1997. Three-dimensional piezoelectric boundary elements. Ph.D. Thesis, Purdue University, USA.

Kumar, S., Singh, R.N., 1996. Crack propagation in piezoelectric materials under combined mechanical and electrical loadings. Acta Materialia 44, 173–200.

Lekhnitskii, S.G., 1963. Theory of Elasticity of an Anisotropic Elastic Body. Holden-Day, New York.

McHenry, K.D., Koepke, B.G., 1983. Electric fields effects on subcritical crack growth in PZT-4. In: R.C. Bradt, D.P. Hasselman, F.F. Lange (Eds.), Fracture Mechanics of Ceramics, vol. 5, pp. 337–352.

Mikhailov, G.K., Parton, V.Z., 1990. Electromagnetoelasticity. Hemisphere, New York.

Pak, Y.E., 1990. Crack extension force in a piezoelectric material. Journal of Applied Mechanics 57, 647–653.

Pak, Y.E., 1992. Linear electro-elastic fracture mechanics of piezoelectric materials. International Journal of Fracture 54, 79–100.

Park, S.B., Park, S.S., Carman, G.P., Hahn, H.T., 1998. Measuring strain distribution during mesoscopic domain reorientation in ferroelectric material. Journal of Engineering Materials and Technology, Transactions of ASME 120, 1–6.

Park, S.B., Sun, C.T., 1995a. Fracture criteria for piezoelectric ceramics. Journal of the American Ceramic Society 78, 1475–1480 (and correction, 1996).

Park, S.B., Sun, C.T., 1995b. Effect of electric fields on fracture of piezoelectric ceramics. International Journal of Fracture 70, 203–216.

Parton, V.Z., 1976. Fracture mechanics of piezoelectric materials. Acta Astronaunt 3, 671–683.

Parton, V.Z., Kudryavtsev, B.A., 1988. Electromagnetoelasticity. Gordon and Breach Science Publishers, New York.

Polovinkina, I.B., Ulitko, A.F., 1978. On the equilibrium of piezoceramic bodies containing cracks. TN 18, 10–17.

Singh, R.N., Wang, H., 1995. Adaptive materials systems. In: G.P. Carman, C. Lynch, N. R. Scottos (Eds.), Proceedings of AMD-vol. 206/MD-vol. 58, ASME, pp. 85–95.

Sosa, H.A., 1991. Plane problems in piezoelectric media with defects. International Journal of Solids and Structures 28, 491–505.

Sosa, H., Khutoryansky, N., 1996. New developments concerning piezoelectric materials with defects. International Journal of Solids and Structures 33, 3399–3414.

Suo, Z., Kuo, C.M., Barnett, D.M., Willis, J.R., 1992. Fracture mechanics for piezoelectric ceramics. Journal of the Mechanics and Physics of Solids 40, 739–765.

Xu, X.-L., Rajapakse, R.K.N.D., 1999. Analytical solution for an arbitrarily oriented void/crack and fracture of piezoceramics. Acta Materialia 47, 1735–1747.

Zhang, T.-Y., Qian, C.-F., Tong, P., 1998. Linear electro-elastic analysis of a cavity or a crack in a piezoelectric material. International Journal of Solids and Structures 35, 2121–2149.

Zhang, T.-Y., Tong, P., 1996. Fracture mechanics for a mode III crack in a piezoelectric material. International Journal of Solids and Structures 33, 343–359.